

1 Performances of One-Dimensional Sonomyography and Surface
2 Electromyography in Tracking Guided Patterns of Wrist Extension

3
4 Jing-Yi Guo¹, Yong-Ping Zheng^{1,2}, Qing-Hua Huang¹, Xin Chen¹, Jun-Feng He¹,
5
6 Helen Lai-Wa Chan³

7
8 ¹Department of Health Technology and Informatics, ²Research Institute of Innovative
9 Products and Technologies, ³Department of Applied Physics, The Hong Kong
10 Polytechnic University, Kowloon, Hong Kong, China

11
12
13
14 Corresponding author:

15 Dr. Yongping Zheng

16 Address: Department of Health Technology and Informatics

17 The Hong Kong Polytechnic University

18 Kowloon, Hong Kong SAR, China

19 Tel: +852 27667664

20 Fax: +852 23624365

21 Email: ypzheng@ieee.org

22

23

24

25 **Abstract**

26 Electromyography (EMG) and ultrasonography have been widely used for skeletal
27 muscle assessment. Recently, it has been demonstrated that the muscle thickness change
28 collected by ultrasound during contraction, namely sonomyography (SMG), can also be
29 used for assessment of muscles and has the potential for prosthetic control. In this study,
30 the performances of one-dimensional sonomyography (1-D SMG) and surface EMG
31 (SEMG) signal in tracking the guided patterns of wrist extension were evaluated and
32 compared, and the potential of 1-D SMG for skeletal muscle assessment and prosthetic
33 control was investigated. Sixteen adult normal subjects including eight males and eight
34 females participated in the experiment. The subject was instructed to perform the wrist
35 extension under the guidance of displayed sinusoidal, square and triangular waveforms at
36 movement rates of 20, 30, 50 cycles per minute. SMG and SEMG root mean squares
37 (RMS) were collected from the extensor carpi radialis respectively and their RMS errors
38 in relation to the guiding signals were calculated and compared. It was found that the
39 mean RMS tracking errors of SMG under different movement rates were $18.9 \pm 2.6\%$
40 (mean \pm SD), $18.3 \pm 4.5\%$, and $17.0 \pm 3.4\%$ for sinusoidal, square, and triangular guiding
41 waveforms, while the corresponding values for SEMG were $30.3 \pm 0.4\%$, $29.0 \pm 2.7\%$, and
42 $24.7 \pm 0.7\%$, respectively. Paired t-test showed that the RMS errors of SMG tracking were
43 significantly smaller than those of SEMG. Significant differences in RMS tracking errors
44 of SMG among the three movement rates ($p < 0.01$) for all the guiding waveforms were
45 also observed using one-way ANOVA. The results suggest that SMG signal, based on
46 further improvement, has great potential to be an alternative method to SEMG to evaluate
47 muscle function and control prostheses.

48 **Keywords-** ultrasound, sonomyography, SMG, electromyography, EMG, muscle,
49 prosthetic control

50

51 **INTRODUCTION**

52 Both electromyography (EMG) and ultrasonography have been widely used to detect
53 the skeletal muscle properties and movements during static and dynamic contractions.
54 EMG describes the bioelectrical properties of skeletal muscles and reveals the
55 physiological process of the muscle contraction. It is generated by the irregular
56 discharges of active motor unit (MU) during the muscle activation (Zwarts and Stegeman
57 2003). The root mean square (RMS) magnitude of EMG is commonly used to describe
58 the time-domain information of EMG signal (Karlsson and Gerdle 2001). However,
59 despite its wide applications in different areas, EMG has some inherent limitations. It is
60 difficult for surface EMG to detect the deep muscles non-invasively, due to the fact that
61 the deep muscle EMG may be attenuated more and mixed by the superficial muscle EMG
62 when reaching the skin surface. EMG signals could vary seriously from people to people
63 even performing the same task (Balogh et al. 1999) and be influenced by many factors,
64 such as muscle cross talk (De Luca 2002), and interelectrode distance (Alemu et al. 2003).
65 In addition, commercially available upper-limb externally powered prosthetic devices
66 using EMG are still limited to one or few degrees of freedom (DoFs) (Zecca et al. 2002).
67 On the other hand, some alternative approaches have been investigated to generate
68 signals for control purposes, including surface electroencephalography (EEG) (Heasman
69 et al. 2002), collected using embedded neurochip implants (Nicoletis 2001; Taylor et al.
70 2002); acoustic signals generated by muscles (Oster 1984; Bolton et al. 1989; Orizio et al.
71 1993), muscle dimensional change (Almstrom and Kadefors 1972; Kenny et al. 1999),

72 and tendon motions (Abboudi et al. 1999; Curcie et al. 2001), etc. These methods each
73 have their own advantages and shortcomings and researchers in this field are still working
74 hard to achieve signals for a better prosthetic control, such as to reduce the cognitive
75 effort required of users, to provide direct feedback when performing movement, and to
76 increase the number of degrees of freedom (DoFs).

77 Ultrasonography is another widely used method to measure muscle morphology
78 change and it has been used together with EMG to provide more comprehensive
79 information about the muscle activities and properties (Whittaker et al., 2007).
80 Researchers using ultrasound images have successfully detected the changes of muscle
81 thickness (Sallinen et al. 2008), pennation angle (Mahlfeld et al. 2004), cross-sectional
82 areas (Reeves et al. 2004) and muscle fascicle length (Fukunaga et al. 2001) in both static
83 and dynamic conditions. Since skeletal muscle architecture is closely correlated with its
84 function (Lieber and Friden 2000), the ultrasound parameters have been employed to
85 characterize muscle activities (Maganaris et al. 2001; Mademli and Arampatzis 2005). In
86 addition, it has been reported that the relationship between EMG and the muscle
87 morphological changes extracted from ultrasound is almost linear only in lower range of
88 forces, but not in higher range of forces for tibialis anterior (Hodges et al. 2003), biceps
89 brachii (Hodges et al. 2003; Shi et al. 2008), transversus abdominis (Hodges et al. 2003;
90 McMeeken et al. 2004), masseter muscle (Georgiakaki et al. 2007), etc.

91 We have recently proposed to use the real-time change of muscle thickness detected
92 using ultrasound, namely sonomyography (SMG), for the prosthetic control (Zheng et al.
93 2006) and the assessment of muscle fatigue (Shi et al. 2007), isometric muscle
94 contraction (Shi et al. 2008), and dynamic muscle contraction (Huang et al. 2007; Guo et

95 al. 2008). The real-time signal about the muscle thickness change during its contraction
96 detected using A-mode ultrasound was named as one-dimensional sonomyography (1-D
97 SMG). In this study, we compared the performances of 1-D SMG signal and surface
98 EMG signal in tracking the waveforms being displayed during the guided movement of
99 wrist extension in term of tracking accuracy. We hypothesized that 1-D SMG signal
100 could better follow the guided waveforms, thus may have potential as a non-invasive
101 method to detect skeletal muscle activities in vivo and to prosthetic control.

102 **METHODS**

103 *A. Subjects*

104 Sixteen healthy adults, including eight males (mean \pm SD age= 26.3 \pm 3.4 years; body
105 weight = 70.3 \pm 11.9 kg; height =172.9 \pm 8.5 cm) and eight females (mean \pm SD age =23.5
106 \pm 1.2 years; body weight = 50.4 \pm 4.1 kg; height = 160.3 \pm 1.7 cm), volunteered to
107 participate in this study and were tested within a period of two months. All the
108 participants were right-hand-dominant without any known neuromuscular disorders. The
109 human subject ethical approval was obtained from the relevant committee in the authors'
110 institution and informed consents were obtained from all subjects prior to the experiment.

111 *B. Data acquisition and processing*

112 An ultrasound pulser/receiver (model 5052 UA, GE Panametrics, Inc. West Chester,
113 OH, USA) was used to drive a 10 MHz single element ultrasound transducer (model
114 V129, GE Panametrics, Inc., West Chester, OH, USA), and to amplify the received
115 signals. The A-mode ultrasound signal was digitized by a high speed A/D converter card

116 with a sampling rate of 200 MHz (Gage CS82G, Gage Applied Technologies, Inc,
117 Canada). The surface EMG signal, captured from the EMG bipolar Ag-AgCl electrodes
118 (Axon System, Inc., NY, USA), was amplified by a custom-designed EMG amplifier
119 with a gain of 1000 and filtered by a 10-300 Hz band-pass analog filter within the
120 amplifier, and then digitized by a data acquisition card (NI-DAQ 6024E, National
121 Instruments Corporation, Austin, TX, USA) with a sampling rate of 4 KHz. The A-mode
122 ultrasound signal was saved frame by frame together with surface EMG for subsequent
123 analysis in a PC with 2.8 GHz Pentium IV microprocessor and 512 MB RAM. The frame
124 rate of A-mode ultrasound was approximately 17 Hz, which was also applied to the data
125 rates of SMG and EMG RMS signals.

126 The 10 MHz single element ultrasound transducer (radius 3 mm) was inserted into a
127 custom-designed holder (radius 10 mm) made of silicone gel in order to attach the
128 transducer to the skin stably (Fig. 4). The transducer together with the holder was
129 positioned on the skin where the belly of extensor carpi radialis is. Double-sided adhesive
130 tape was used to fixate the holder, while ultrasound gel was imposed between the
131 transducer and skin. The EMG bipolar Ag-AgCl electrodes were attached to the skin
132 surface near the ultrasound transducer and along the extensor carpi radialis muscle. The
133 distance between the two electrodes was approximately 20 mm and an additional
134 electrode for providing the reference electrical signal was placed near the head of ulna.

135 The A-mode ultrasound and surface EMG were collected, stored and analyzed by the
136 software for ultrasound measurement of motion and elasticity (UMME,
137 <http://www.sonomyography.org>) developed using Visual C++. The time delay between
138 the two data collection systems was calibrated using a method similar to that described by

139 Huang et al. (2005, 2007). As the transducer moved cyclically up and down in a water
 140 tank, the two signals representing A-mode ultrasound, and simulated EMG respectively
 141 were collected and stored. The time delay between the data sets was calculated using a
 142 cross-correlation algorithm. The details can be found in our earlier study (Huang et al.
 143 2007).

144 The muscle deformation signal, i.e. SMG, was extracted from the A-mode ultrasound.
 145 A cross-correlation algorithm was employed to track the displacements of upper and
 146 lower boundaries of extensor carpi radialis muscle during the wrist extension. The
 147 equation used to calculate the normalized one-dimensional cross-correlation is as follow:

$$148 \quad R_{.xy} = \frac{\sum_{i=0}^{N-1} [x(i) - \bar{X}][y(i) - \bar{Y}]}{\sqrt{\sum_{i=0}^{N-1} [x(i) - \bar{X}]^2 \sum_{j=0}^{N-1} [y[j] - \bar{Y}]^2}} \quad (1)$$

149 Where \bar{X} and \bar{Y} are the means of $x(i)$ and $y(j)$, respectively. It requires a reference
 150 signal from an initial frame and would search for the signal most similar to the reference
 151 signal for estimating the object position in the updated frame. The A-mode ultrasound
 152 echoes reflected from the fat-muscle and muscle-bone interfaces were selected by two
 153 tracking windows (Fig. 2c) in the first frame. When the muscle was contracting, its
 154 dimensional changes induced the variations of distance between the interface of fat-
 155 muscle and that of muscle-bone, which would cause the A-mode ultrasound echoes to
 156 shift for a certain distance. The percentage deformation of the muscle is defined as

$$157 \quad D = \frac{(d - d_0)}{d_0} \times 100\% \quad (2)$$

158 Where d_0 is the initial distance between the two echoes and d is the distance when the

159 muscle is contracting.

160 The RMS amplitude of EMG was calculated and compared with the SMG signal to
161 investigate which one could better follow the guiding waveforms during the wrist
162 extension.

163

164 *C. Experiment protocol*

165 Before the experiment formally began, all the subjects were trained for two or three
166 trials to make sure they were familiar with the experimental protocol. None of subject had
167 been trained before. Both 1-D SMG and surface EMG signals were tested for their
168 accuracy in following the displayed waveform patterns. As shown in Fig. 1, the subject
169 was seated comfortably in an adjustable chair with his/her trunk fixed by a strap onto the
170 back of the chair to prevent posture change during the test and the right forearm resting
171 on the table with pronation. The elbow was flexed at approximately 140 degree between
172 the upper arm and forearm. The angle between the upper arm and trunk was
173 approximately 30 degrees. The subject was instructed to perform wrist extension under
174 the guidance of displayed sinusoidal (Fig. 2a), square (Fig. 2d) and triangular waveforms
175 (Fig. 2e) respectively. The order of the experiments was randomly selected for each
176 subject. For the SMG test, the subject was required to perform several wrist extensions
177 before each experiment in order to determine the amplitude of the muscle deformation
178 signal extracted from A-mode ultrasound (i.e. 1-D SMG), and the amplitudes of the
179 guiding waveforms were adjusted based on the obtained muscle deformation range.
180 During the experiments, the subjects were encouraged to try their best to produce real-
181 time muscle deformation signal, i.e. SMG, the same as the waveform being displayed on

182 the screen by adjusting the range of their wrist movement in response to the visual
183 feedback from the guiding waveforms. If the muscle deformation signal generated did not
184 follow the guiding waveform well, the subjects could adjust the strength of their muscles
185 in order to match the two waveforms better. The wrist extension rates were set to be 20,
186 30, 50 cycles per minute for each guiding waveform. Therefore, every subject totally
187 performed nine tasks of wrist extension for the three different movement patterns
188 (sinusoidal, square and triangular waveforms) for SMG tests (Fig. 2). Three repeated
189 trials were performed for each task and there was a rest of 3 minutes between two
190 adjacent trials to avoid muscle fatigue. The A-mode ultrasound signals were saved in the
191 PC hard disk for further analysis. To make the system response time comparable to the
192 subsequent EMG test, the EMG signals were also collected and analyzed during the
193 ultrasound measurement but the EMG RMS signal was not displayed and the results not
194 used.

195 The subjects were also instructed to perform another set of wrist extension tasks, using
196 the RMS of their surface EMG signals to follow the reference waveforms. Similar testing
197 protocol was adopted as that in the SMG test. To make the results comparable, during the
198 EMG test, the A-mode ultrasound signals were collected and analyzed in real-time but
199 the SMG signal was not displayed, as shown in Fig. 3. The subjects could adjust the
200 range of wrist movement according to the real-time display of their EMG RMS signals to
201 better fit the reference signal. Totally nine tasks of wrist extension for surface EMG test
202 under the three wrist extension rates for the three different waveforms were performed by
203 each subject. Figure 3 shows the interface of the software to collect the data of EMG
204 RMS and the three types of guiding waveforms.

205 *D. Data analysis*

206 The SMG and EMG RMS data were respectively normalised by expressing measures
207 as a percentage of the largest SMG and EMG RMS signals detected any time during the
208 testing procedure. The RMS tracking errors (RMSTE) between SMG/EMG RMS and the
209 corresponding guiding waveforms were calculated separately, defined as:

$$210 \quad \text{RMSTE} = \sqrt{\frac{1}{N} \sum_{n=1}^N (\text{Sig}_1(n) - \text{Sig}_2(n))^2} \quad (3)$$

211 where $\text{Sig}_1(n), \text{Sig}_2(n)$ are signals with N points of values.

212 The performances of SMG and EMG RMS to follow the three guiding waveform
213 patterns were compared using paired t-test. One-Way ANOVA was also used to
214 determine whether there were any differences in the performances of the SMG signals
215 under the three different movement rates. All the data were calculated using Minitab
216 (Minitab Inc., Pennsylvania, USA). Statistical significance was set at the 5% probability
217 level.

218 **RESULTS**

219 Totally 432 data sets were recorded from the sixteen subjects. Table 1 summarizes the
220 RMS tracking errors of SMG and EMG for the three guiding waveform patterns under
221 different movement rates. The overall mean RMS tracking errors of SMG under the three
222 movement rates were $18.9 \pm 2.6\%$ (mean \pm S.D.), $18.3 \pm 4.5\%$, and $17.0 \pm 3.4\%$ for the
223 sinusoid, square, and triangle guiding waveforms, while the corresponding values for
224 EMG were $30.3 \pm 0.4\%$, $29.0 \pm 2.7\%$, and $24.7 \pm 0.7\%$, respectively (Fig. 5). Paired t-test

225 revealed that the overall mean RMS tracking error of SMG was significantly smaller than
226 that of EMG for all the three guiding waveforms.

227 One-way ANOVA showed that there were significant differences in the RMS
228 tracking errors of SMG among the three wrist extension rates ($p < 0.01$) for all the three
229 guiding waveforms as demonstrated in Fig. 6. An apparent increasing trend of the RMS
230 tracking error using SMG was observed with the increase of the movement rate for all the
231 different guiding patterns. However, for EMG, statistical analysis revealed that the RMS
232 tracking error was significantly different among the three movement rates only for the
233 square waveform ($P = 0.001$), but not for sinusoid ($P = 0.921$) and triangle ($P = 0.762$)
234 waveforms. As shown in Fig. 7, the RMS tracking error for EMG generally showed
235 smaller variations under different rates of wrist extension.

236 **DISCUSSION**

237 In this paper, we investigated the performances of surface EMG and 1D SMG, i.e.
238 real-time muscle thickness change detected using A-mode ultrasound, in tracking three
239 different movement patterns of the wrist extension guided by waveforms shown on the
240 PC screen. We found that the tracking errors of SMG under different wrist extension
241 rates (ranged from $14.0 \pm 1.9\%$ to $23.3 \pm 3.7\%$) were statistically significantly smaller than
242 the corresponding values of surface EMG (ranged from $24.2 \pm 4.4\%$ to $32.1 \pm 4.1\%$) for all
243 the movement patterns studied (Fig. 5 and Table 1), indicating that SMG performed
244 better than surface EMG in following the given movement patterns in term of tracking
245 accuracy.

246 For decades, EMG signal has been widely used in the areas of muscle fatigue
247 (Masuda et al. 1998; Fukuda et al. 2006), muscle pathology (Haig et al. 1996; Hogrel
248 2005; Labarre et al. 2006; Ohata et al. 2006), prosthetic device control (Kermani et al.
249 1995; Boostani and Moradi 2003; Soares et al. 2003), and athlete muscle assessment
250 under different postures (Worrell et al. 1992). Some researchers have demonstrated that
251 the relationship between EMG and the force of the related joint was not linear (Alkner et
252 al. 2000). Whereas, in our previous study, it was shown that the SMG signal was linear
253 with the torque generated by biceps brachii muscles (Shi et al. 2008). These results may
254 indicate that SMG signal may have a more direct, simple correlation (linear) with the
255 torque generated by the corresponding muscle. The results of this study further
256 demonstrate the potentials for SMG to serve as a feedback of rehabilitation of muscle
257 dysfunction and assessment of muscle activity..

258 Compared with surface EMG, the main advantage of SMG is that ultrasound can
259 inherently detect individual muscle at neighbouring locations and different depths
260 without the effects of muscle cross talk by using one or more ultrasound transducers. Due
261 to the challenges in separating SEMG signals generated by different neighbouring
262 muscles, i.e. cross talk, the available prostheses controlled by SEMG could only provide
263 limited number of DoFs. By using multi-channels of SMG signal, it is possible to realize
264 the control of prostheses with multiple DoFs. It may benefit the users with more grasping
265 functions and less training efforts.

266 Further studies are required to demonstrate these advantages quantitatively. It is also
267 very interesting to further investigate whether the good performance of SMG on the
268 extensor carpi radialis muscle for wrist control observed in this study can be applied to

269 other skeletal muscles. A follow-up study using SMG to control real powered prostheses
270 with a hand open-close feature is being conducted in our group. It has already been
271 demonstrated that the muscles of residual limbs could generated SMG as well (Zheng et
272 al. 2006).

273 It is interesting to explore why SMG could perform significantly better than EMG in
274 tracking different given movement patterns of the joint under different movement rates. It
275 has been reported that there is an exponential relationship between EMG magnitudes and
276 the strengths generated by different skeletal muscles (Deluca 1997; Hodges et al. 2003;
277 Zheng et al. 2006; Shi et al. 2008). We have previously found that SMG signals of a
278 skeletal muscle have approximately linear relationships with the strengths generated by
279 this muscle, represented either by torques for isometric contractions (Shi et al. 2008) or
280 by joint angles for isotonic contractions (Zheng et al. 2006). It appears that SMG and the
281 corresponding joint angle follow a relatively simple relationship in comparison with the
282 relation between EMG and joint angle. The results of this and previous studies appear to
283 imply that the architectural changes during muscle contraction relate more directly to the
284 actuation achieved (mechanical output), while the EMG is a measure of activation
285 intended (electrical input). In relation to the findings of the present study, we may
286 interpret that our motor control and visual feedback system could perform better when the
287 control signal has a linear relationship with the target signal to control, which is the wrist
288 angle in this case. This may probably reduce the training efforts when the SMG signal is
289 used for the prosthetic control. Further studies are required to study how many training
290 efforts can be saved when using SMG for control instead of EMG. More normal and
291 residual limbs should be tested to ensure a solid conclusion.

292 As expected, it was found that as the movement rates increased, the tracking errors of
293 SMG increased (Fig. 6). When the movement rates increased, the subjects were required
294 to perform the same movement in a shorter time period. Furthermore, according to
295 subjects' verbal reports, the visual feedback used to provide instantaneous performance
296 indication during the test slightly distracted their attention. Thus, as the movement rates
297 increased, the possibility for SMG to "move away" from the guiding waveform may also
298 increase, resulting in higher tracking errors. However, this increasing trend in tracking
299 error with the increase of movement rate was not observed in EMG RMS (Fig. 7). It was
300 also noted that the performance of SMG tracking at the highest rate was still better than
301 the best performance of the EMG tracking among all the tests. The reducing performance
302 of SMG induced by the increase of movement speed may have a number of potential
303 reasons. First, the frame rate of A-mode ultrasound (approximately 17 Hz), which also
304 determines how fast the data points of SMG signal are given, was relatively low in the
305 study. With the increase of the wrist flexion-extension rate, the SMG data collected in
306 each cycle would be reduced. Therefore, the subject may have fewer data points to refer
307 to for following the given waveform. Since we have also controlled the data rate of EMG
308 RMS to 17 Hz during the test, this effect should have affected the performance of EMG
309 tracking as well when the movement speed was increased, however, it was not observed
310 in this study. A higher frame rate system could be used to further investigate the effect of
311 data collection speed in future studies. The second possible reason is that SMG is a signal
312 not only related to the bioelectrical properties of muscles, i.e. how muscles are activated,
313 but also dependent on the mechanical properties of muscle-tendon complex, i.e.
314 viscoelastic properties. With the increase of the muscle contraction speed, the hysteresis

315 of SMG signal may also increase. This will make it more challenging for the subjects to
316 follow the given movement patterns using SMG signal. However, EMG signals would
317 not be affected by this effect, as they are more related to bioelectrical properties of
318 muscles. Again, further studies are required to better understand the effects of the
319 viscoelasticity of muscles and other tissues on the generation and applications of SMG
320 signal.

321 In summary, we demonstrated in this study that SMG signal obtained using A-mode
322 ultrasound could provide better performance flexion-extension of wrist in comparison
323 with EMG in tracking different given patterns under different wrist flexion-extension
324 rates. The use of single element transducer in A-mode image allowed great flexibility in
325 designing SMG sensor, thus it is practically feasible to attach such a probe on the skin
326 surface conveniently for the purposes of control or muscle function evaluation, similar to
327 the use of surface EMG. However, further studies are required to verify the
328 performances of SMG signals on different muscles under different conditions. The
329 mechanism of how the increasing movement rate of wrist affects the SMG tracking
330 performances should also be further investigated.

331 **ACKNOWLEDGMENTS**

332 This work was supported by The Hong Kong Polytechnic University (G-YE22, 1-BB69)
333 and the Grant Council of Hong Kong (PolyU 5331/06E).

334 **REFERENCES**

335 Abboudi RL, Glass CA, Newby NA, Flint JA, Craelius W. A biomimetic controller for a
336 multifinger prosthesis. *IEEE T Rehabil Eng* 1999;7:121–129.

337 Alemu M, Kumar DK, and Bradley A. Time-frequency analysis of SEMG - with special
338 consideration to the interelectrode spacing. *IEEE Trans Neural Syst Rehabil Eng*
339 2003;11:341-345.

340 Alkner BA, Tesch PA, Berg HE. Quadriceps EMG/force relationship in knee extension
341 and leg press. *Med Sci Sports Exerc* 2000; 32:459-63.

342 Almstrom C, Kadefors R. Methods for transducing skin movements in the control of
343 assistive devices. In: *Proceedings of Third International Conference on Medical*
344 *Physics*. 1972. vol. 33. Sweden pp. 2.

345 Balogh I, Hansson GA, Ohlsson K, Stromberg U, Skerfving S. Interindividual
346 variation of physical load in a work task. *Scand J Work Env Hea* 1999;25:57-66.

347 Bolton CF, Parkers A, Thompson TR, Clark MR, Sterne CJ. Recording sound from
348 human skeletal muscle: technical and physiological aspects. *Muscle Nerve* 1989;12:
349 126-134.

350 Boostani R, Moradi MH. Evaluation of the forearm EMG signal features for the control
351 of a prosthetic hand. *Physiol Meas* 2003;24:309-319.

352 Curcie DJ, Flint JA Craelius W. Biomimetic finger control by filtering of distributed
353 forelimb pressures. *IEEE Trans Neural Syst Rehabil Eng* 2001;9:69-75.

354 De Luca CJ. The use of surface electromyography in biomechanics. *J Appl Biomech*
355 1997;13:135-163.

356 De Luca CJ. *Surface electromyography: detection and recording*. Boston: DelSys Inc,
357 2002.

358 Fukuda K, Umezu Y, Shiba N, Tajima F, Nagata K. Electromyographic fatigue analysis
359 of back muscles during remote muscle contraction. *J Back Musculoskelet*
360 2006;19:61-66.

361 Fukunaga T, Kubo K, and Kawakami Y. In vivo behaviour of human muscle tendon
362 during walking. *Proc Biol Sci* 2001; 268:229-233.

363 Georgiakaki I, Tortopidis D, Garefis P, Kiliaridis S. Ultrasonographic thickness and
364 electromyographic activity of masseter muscle of human females. *J Oral Rehabil*
365 2007; 34:121-128.

366 Guo JY, Zheng YP, Huang QH, Chen X. Dynamic Monitoring of Forearm Muscles Using
367 1D Sonomyography (SMG) System. *J Rehabil Res Dev* 2008; 45: 187-196.

368 Haig AJ, Gelblum JB, Rechtien JJ, Gitter AJ. Technology assessment: the use of surface
369 EMG in the diagnosis and treatment of nerve and muscle disorders. *Muscle Nerve*
370 1996;19:392-395.

371 Heasman JM, Scott TRD, Kirkup L, Flynn RY, Vare VA Gschwind CR. Control of a
372 hand grasp neuoprosthesis using an electroencephalogram-triggered switch:
373 demonstration of improvements in performance using wavepacket analysis. *Med Biol*
374 *Eng Comput* 2002; 40:588–593.

375 Hodges PW, Pengel LHM, Herbert RD, Gandevia SC. Measurement of muscle
376 contraction with ultrasound imaging. *Muscle Nerve* 2003;27:682-692.

377 Hogrel JY. Clinical applications of surface electromyography in neuromuscular disorders.
378 *Neurophysiol Clin* 2005;35:59-71.

379 Huang QH, Zheng YP, Lu MH, and Chi ZR. Development of a portable 3D ultrasound
380 imaging system for musculoskeletal tissues. *Ultrasonics* 2005; 43:153-163.

381 Huang QH, Zheng YP, Chen X, He JF, Shi J. Synchronization between somyography,
382 electromyography and joint angle. *Open Biomed Eng J* 2007;1:77-84.

383 Karlsson S, Gerdle B. Mean frequency and signal amplitude of the surface EMG of the
384 quadriceps muscles increase with increasing torque- a study using the continuous
385 wavelet transform. *J Electromyogr Kinesiol* 2001;11:131-140.

386 Kenney LP, Lisitsa I, Bowker P, Heath GH, Howard D. Dimensional change in muscle
387 as a control signal for powered upper limb prostheses: a pilot study. *Med Eng Phys*
388 1999;21:589-597.

389 Kermani MZ, Wheeler BC, Badie K, Hashemi TM. EMG feature evaluation for
390 movement control of upper extremity prostheses. *IEEE Trans Rehabil Eng*
391 1995;3:324-333.

392 Labarre VA. Assessment of muscle function in pathology with surface electrode EMG.
393 *Rev Neurolvol* 2006;162:459-465.

394 Lieber RL, Friden J. Functional and clinical significance of skeletal muscle architecture.
395 *Muscle Nerve* 2000;23:1647-1666.

396 Mademli L, Arampatzis A. Behaviour of the human gastrocnemius muscle architecture
397 during submaximal isometric fatigue. *Eur J Appl Physiol* 2005;94:611-617.

398 Maganaris CN. Force-length characteristics of in vivo human skeletal muscle. *Acta*
399 *Physiol Scand* 2001;172:279-285.

400 Mahlfeld K, Franke J, Awiszus F. Postcontraction changes of muscle architecture in
401 human quadriceps muscle. *Muscle Nerve* 2004;29:597-600.

402 Masuda K, Masuda T, Sadoyama T, Inaki M, Katsuta S. Changes in surface EMG
403 parameters during static and dynamic fatiguing contractions. *J Electromyogr Kinesiol*
404 1998; 9:39-46.

405 McMeeken JM, Beith ID, Newham DJ, Milligan P, Critchley DJ. The relationship
406 between EMG and change in thickness of transversus abdominis. *Clin Biomech*
407 2004;19:337-342.

408 Nicoletis MAL. Actions from thoughts. *Nature* 2001;409:403–407.

409 Ohata K, Tsuboyama T, Ichihashi N, Minami S. Measurement of muscle thickness as
410 quantitative muscle evaluation for adults with severe cerebral palsy. *Phys Ther*
411 2006;86:1231-1239.

412 Orizio C. Muscle sound: bases for the introduction of a mechnomyographic signal in
413 muscle studies. *Crit Rev Biomed Eng* 1993; 21:201–243.

414 Oster G. Muscle sound. *Sci Am* 1984;250:108–114.

415 Reeves ND, Maganaris CN, Narici MV. Ultrasonographic assessment of human skeletal
416 muscle size. *Eur J Appl Physiol*. 2004; 91:116-118.

417 Sallinen J, Ojanen T, Karavirta L, Ahtiainen JP, Hakkinen K. Muscle mass and strength,
418 body composition and dietary intake in master strength athletes vs untrained men of
419 different ages. *J Sports Med Phys Fitness*. 2008; 48:190-196.

420 Shi J, Zheng YP, Chen X, Huang QH. Assessment of muscle fatigue using
421 sonomyography: Muscle thickness change detected from ultrasound images. *Med*
422 *Eng Phys* 2007;29:472-479.

423 Shi J, Zheng YP, Huang QH, Chen X. Relationships among continuous sonomyography,
424 electromyography and torque generated by normal upper arm muscles during
425 isometric contraction. *IEEE T Bio-Med Eng* 2008; 55:1191-1198.

426 Soares A, Andrade A, Lamounier E, Carrijo R. The development of a virtual Myoelectric
427 prosthesis controlled by an EMG pattern recognition system based on neural
428 networks. *J Intell Inf Syst* 2003;21:127-141.

429 Taylor DM, Tillery SIH, Schwartz AB. Direct cortical control of 3D neuroprosthetic
430 device. *Science* 2002;296:1829–1832.

431 Whittaker J, Teyhen D, Elliott J, Cook K, Langevin H, Dahl H, Stokes M. Rehabilitative
432 Ultrasound Imaging: Understanding the Technology and its Applications. *J Orthop
433 Sports Phys Ther* 2007;37: 435-449.

434 Worrell TW, Corey BJ, York SL, Santiestaban J. An analysis of supraspinatus EMG
435 activity and shoulder isometric force development. *Med Sci Sport Exer*
436 1992;24:744-748.

437 Zecca M, Micera S, Carrozza MC. Control of multifunctional prosthetic hands by
438 processing the electromyographic signal. *Crit Rev Biomed Eng* 2002;30:459-485.

439 Zheng YP, Chan MM, Shi J, Chen X, Huang QH. Sonomyography: Monitoring
440 morphological changes of forearm muscles in actions with the feasibility for the
441 control of powered prosthesis. *Med Eng Phys* 2006;28:405-415.

442 Zwarts MJ, Stegeman DF. Multichannel surface EMG: basic aspects and clinical utility.
443 *Muscle Nerve* 2003;28:1 – 17.

444
445
446
447

448 **Captions of Figures**

449 Fig. 1 The diagram of the data collection system.

450 Fig. 2 The software interface was used to simultaneously collect 1-D SMG, SEMG
451 signals (a) The sinusoidal waveform with a rate of 20 cycles per minute was used to
452 guide the wrist extension movement. The subject used 1-D SMG signal to track the
453 sinusoidal pattern. (b) Surface EMG was also collected for reference. (c) The muscle
454 deformation signal (i.e. SMG) was measured by detecting the distance change between
455 the A-mode ultrasound echoes reflected from the fat-muscle and muscle-bone interfaces,
456 which were selected by two the tracking windows. A cross-correlation algorithm was
457 employed to track the movements of the echoes during the wrist extension. The muscle
458 deformation signal (i.e. SMG) was calculated using the change of the time interval
459 between the echoes and displayed along with the guiding waveform for tracking (a). (d)
460 1-D SMG signal tracks the square waveform with a rate of 30 cycles per minute; (e) 1-D
461 SMG signal tracks the triangular waveform with a rate of 50 cycles per minute.

462 Fig. 3 (a) The software interface was used to collect the SEMG and A-mode ultrasound
463 signals. (a) SEMG signal was collected. (b) The sinusoidal waveform with a rate of 20
464 cycles per minute was used to guide the wrist extension movement. SEMG RMS was
465 calculated to track the sinusoidal pattern. (c) A-mode ultrasound signal was also collected
466 for reference (d) SEMG RMS tracks the square waveform with a rate of 30 cycles per
467 minute; (e) SEMG RMS tracks the triangular waveform with a rate of 50 cycles per
468 minute.

469 Fig. 4 Placement of the 1D ultrasound transducer, SEMG electrodes on the forearm, with
470 ultrasound gel applied between the ultrasound transducer and skin to aid acoustic
471 coupling.

472 Fig. 5 The RMS tracking errors (%) between SMG/SEMG and the guiding waveforms.
473 The error bar represents the standard deviation of the results of three different movement
474 rates.

475 Fig. 6 The tracking errors of SMG for the three guiding waveforms under different
476 movement rates. The error bar represents the standard deviation of the results of the
477 sixteen subjects.

478 Fig. 7 The RMS tracking errors of SEMG under the three different wrist extension rates
479 for different guiding waveforms. The error bar represents the standard deviation of the
480 results of the sixteen different subjects.

481

482

483 **Table 1.** The RMS tracking errors (%) between SMG/surface EMG and the guiding
 484 waveforms at the three movement rates (Mean \pm S.D.) and the mean RMS tracking errors
 485 averaged over the three movement rates for sinusoid, square, and triangle guiding
 486 waveforms.

<i>Rate</i> (Cycles per minute)	<i>SMG</i>			<i>Surface EMG</i>		
	<i>sinusoid</i>	<i>square</i>	<i>triangle</i>	<i>sinusoid</i>	<i>square</i>	<i>triangle</i>
<i>20</i>	16.3 \pm 7.8	14.6 \pm 1.7	14.0 \pm 1.9	30.5 \pm 4.7	27.0 \pm 4.2	24.2 \pm 4.4
<i>30</i>	19.0 \pm 3.0	17.1 \pm 1.6	16.3 \pm 2.5	29.9 \pm 6.4	27.8 \pm 3.0	24.4 \pm 6.3
<i>50</i>	21.5 \pm 3.2	23.3 \pm 3.7	20.7 \pm 3.1	30.6 \pm 5.5	32.1 \pm 4.1	25.4 \pm 4.8
<i>Mean</i>	18.9 \pm 2.6	18.3 \pm 4.5	17.0 \pm 3.4	30.3 \pm 0.4	29.0 \pm 2.7	24.7 \pm 0.7

487

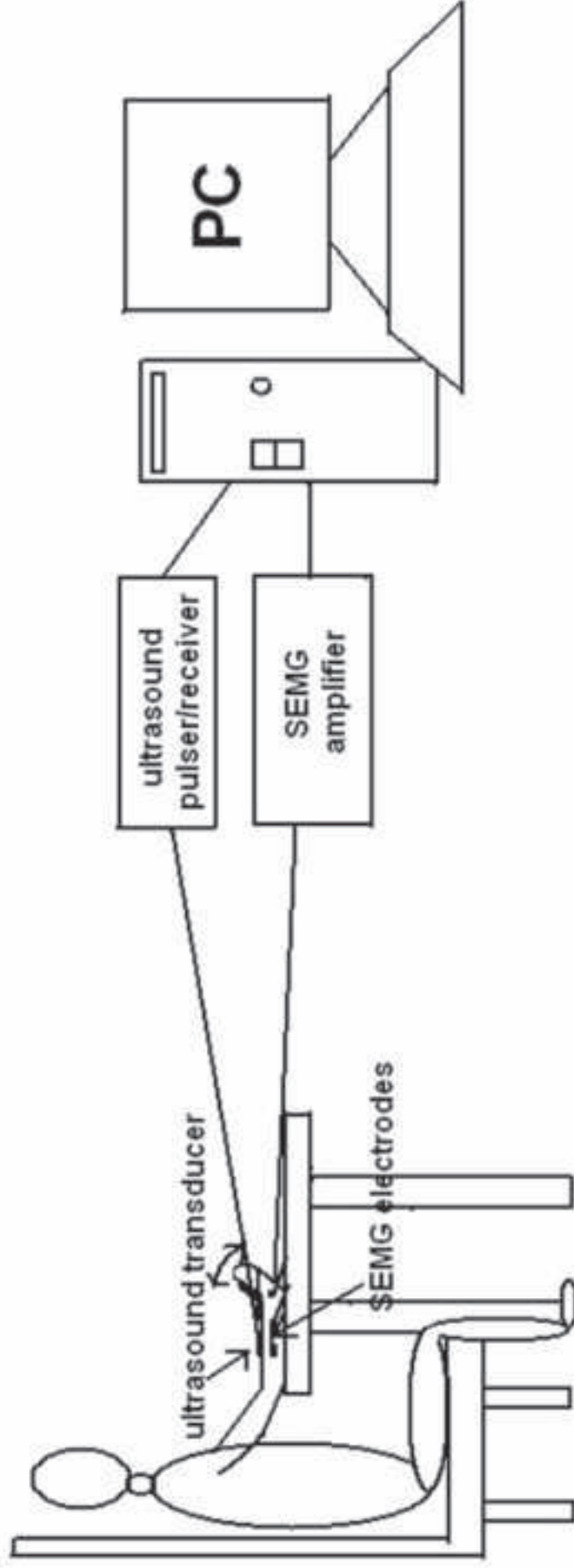


Fig. 1

Figure 2
Click here to download high resolution image

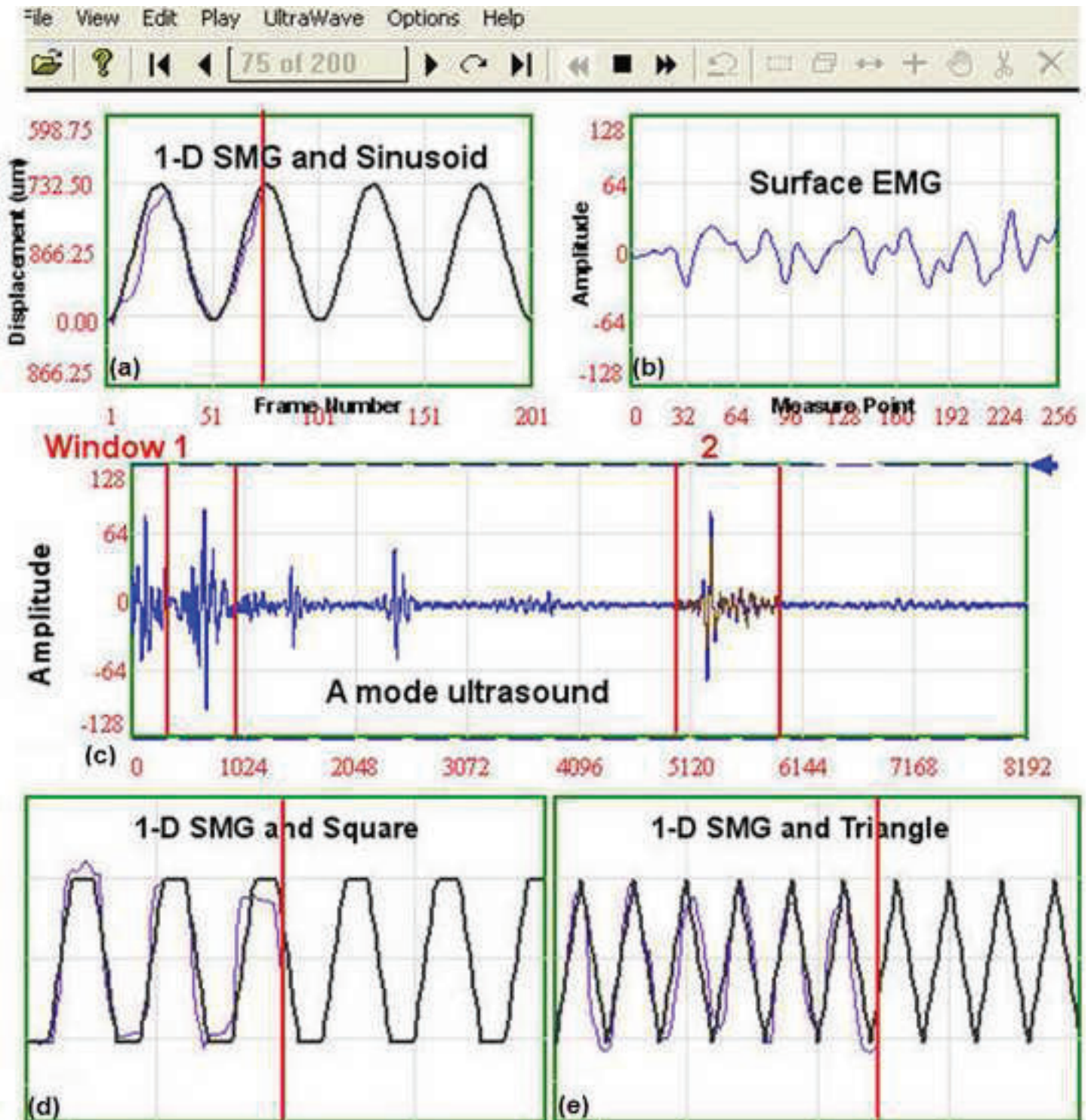


Fig. 2

Figure 3
Click here to download high resolution image

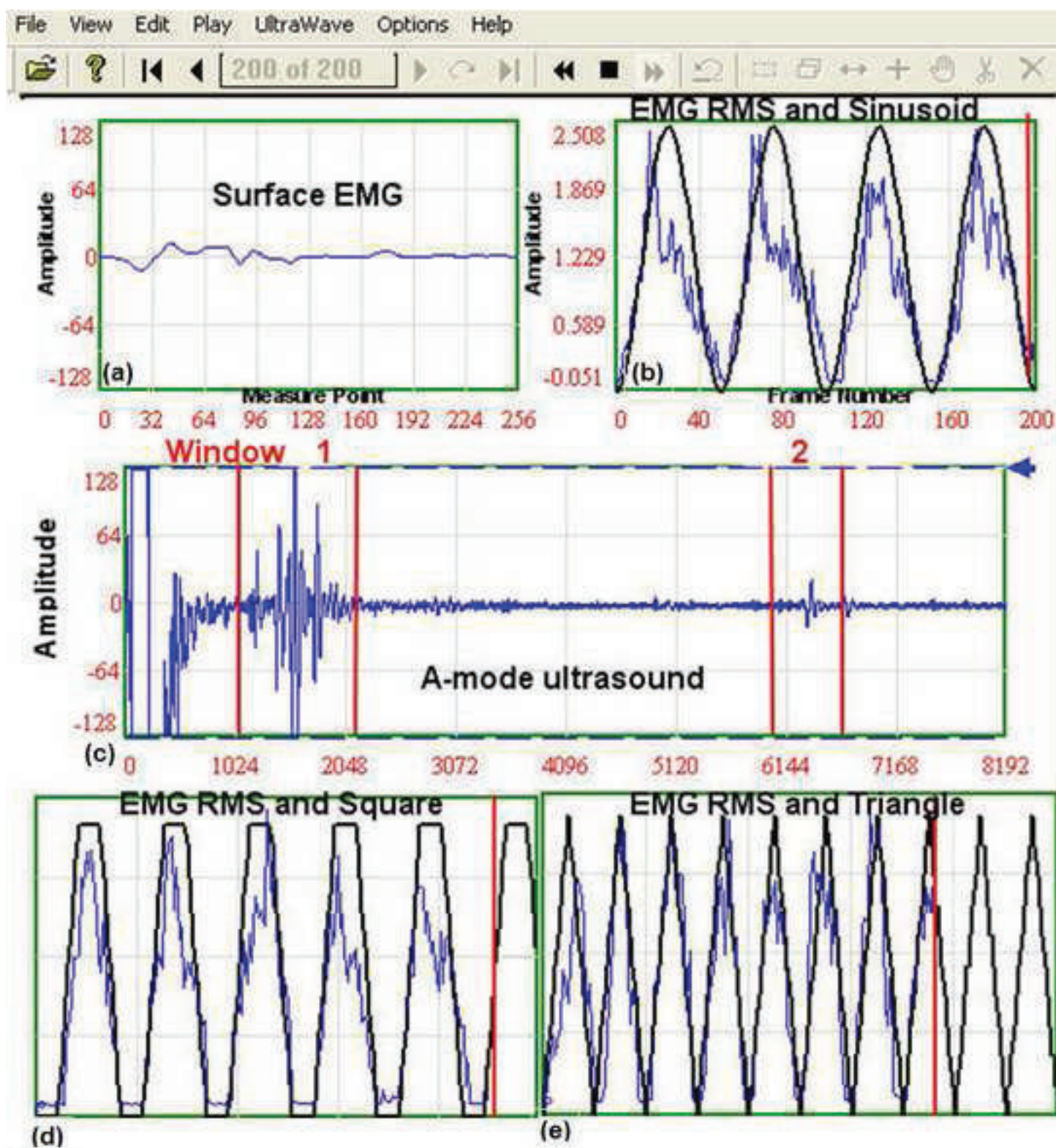


Fig. 3

Figure 4
[Click here to download high resolution image](#)

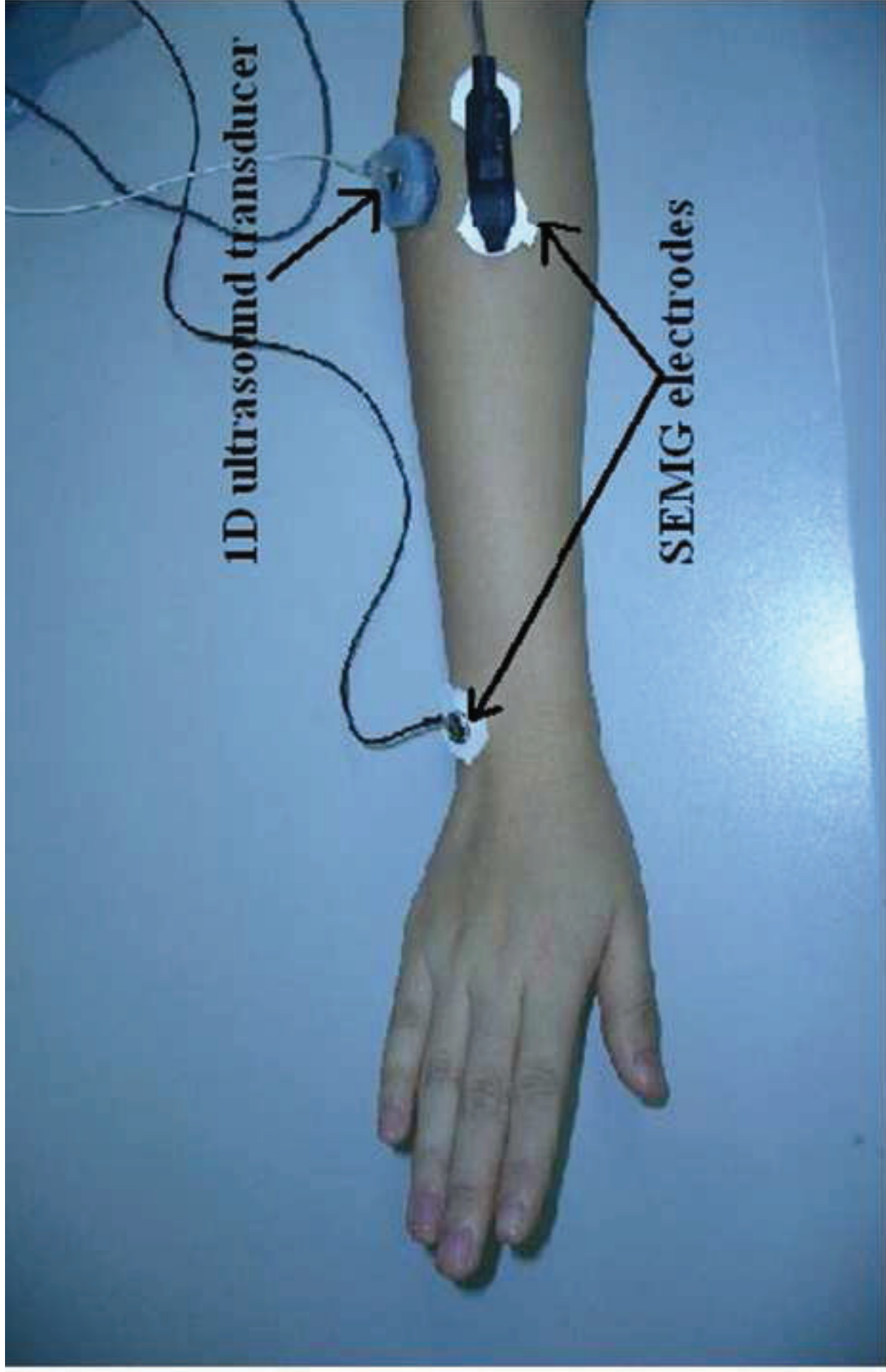


Fig. 4

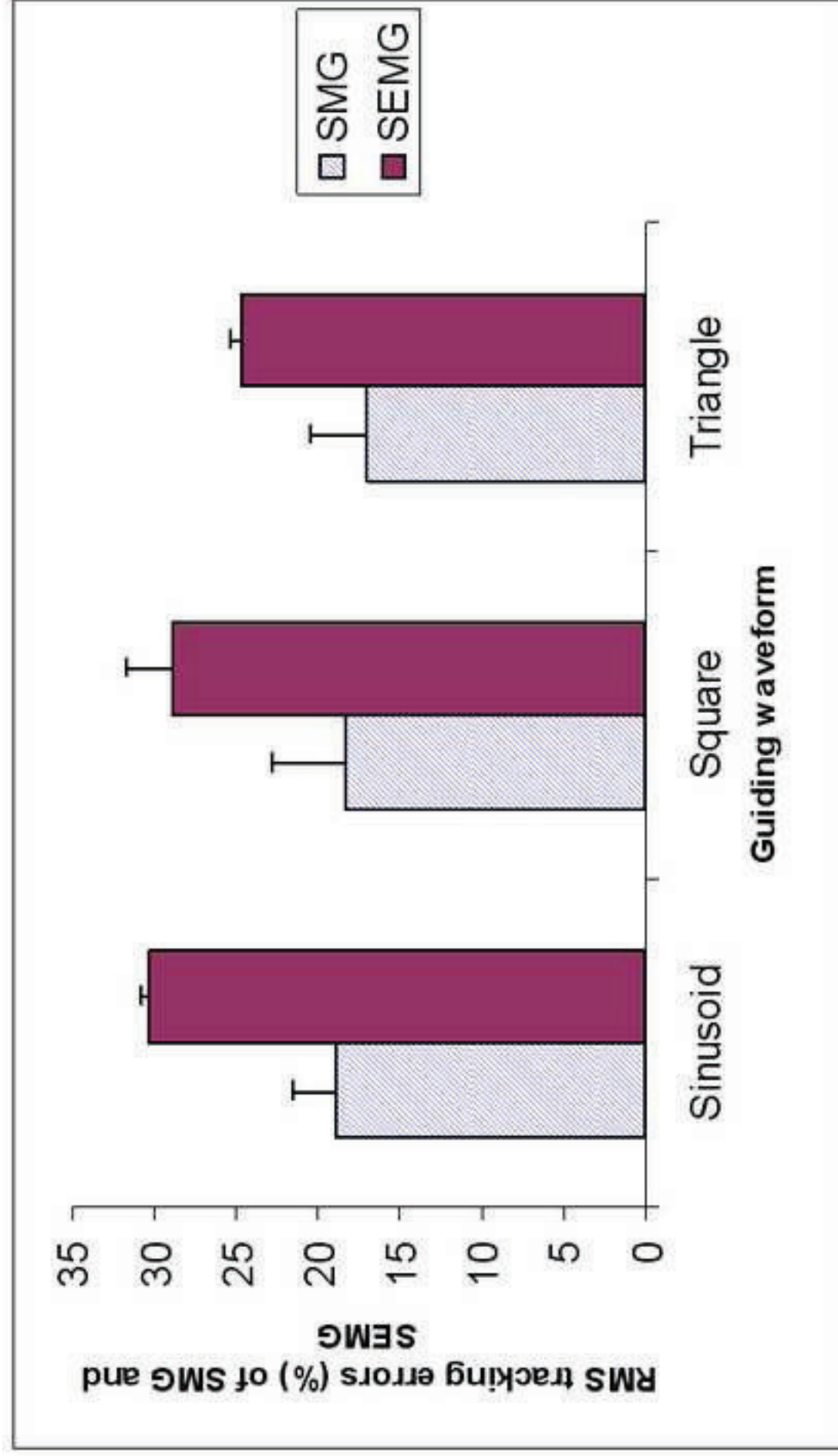


Fig. 5

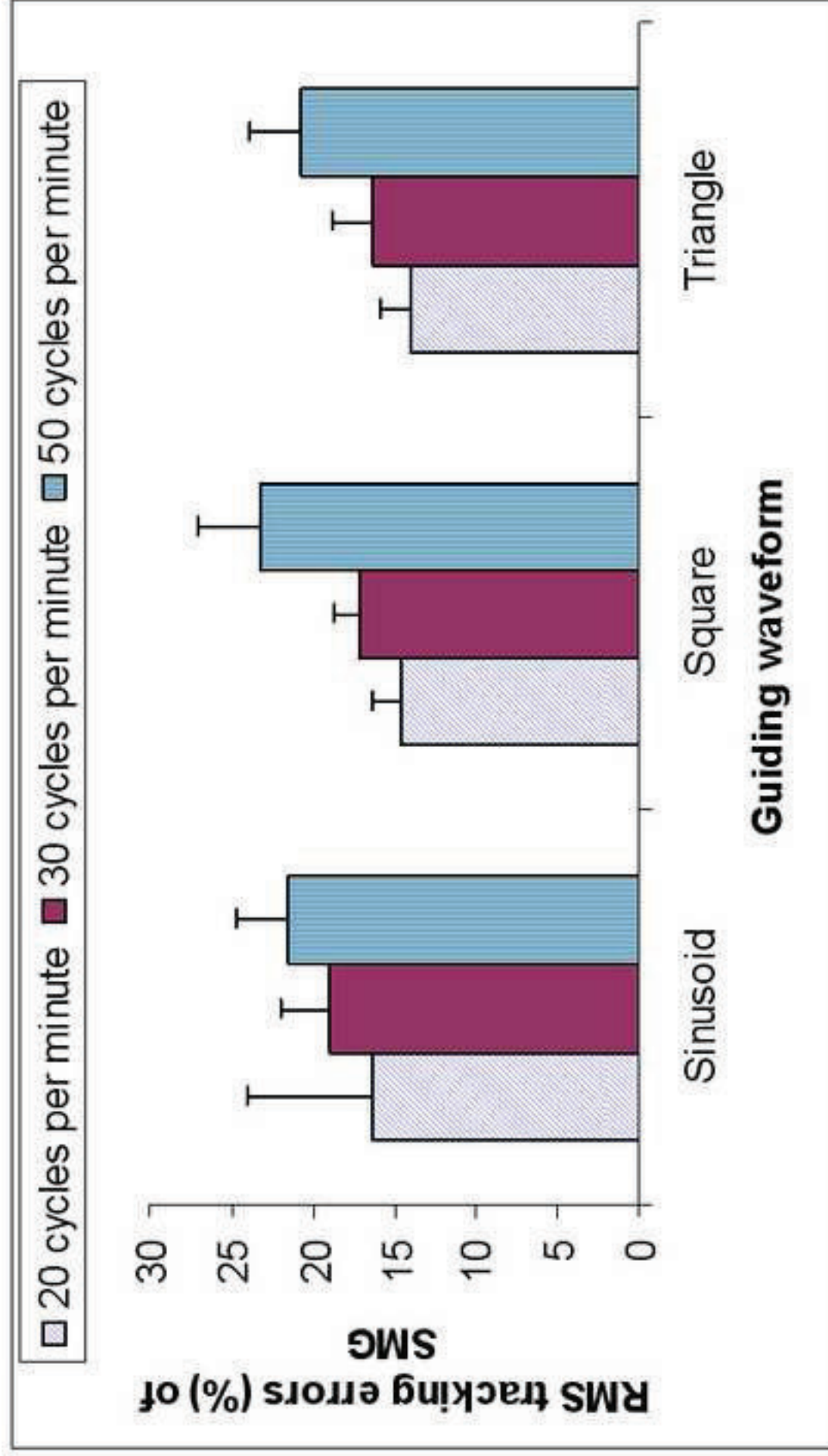


Fig. 6

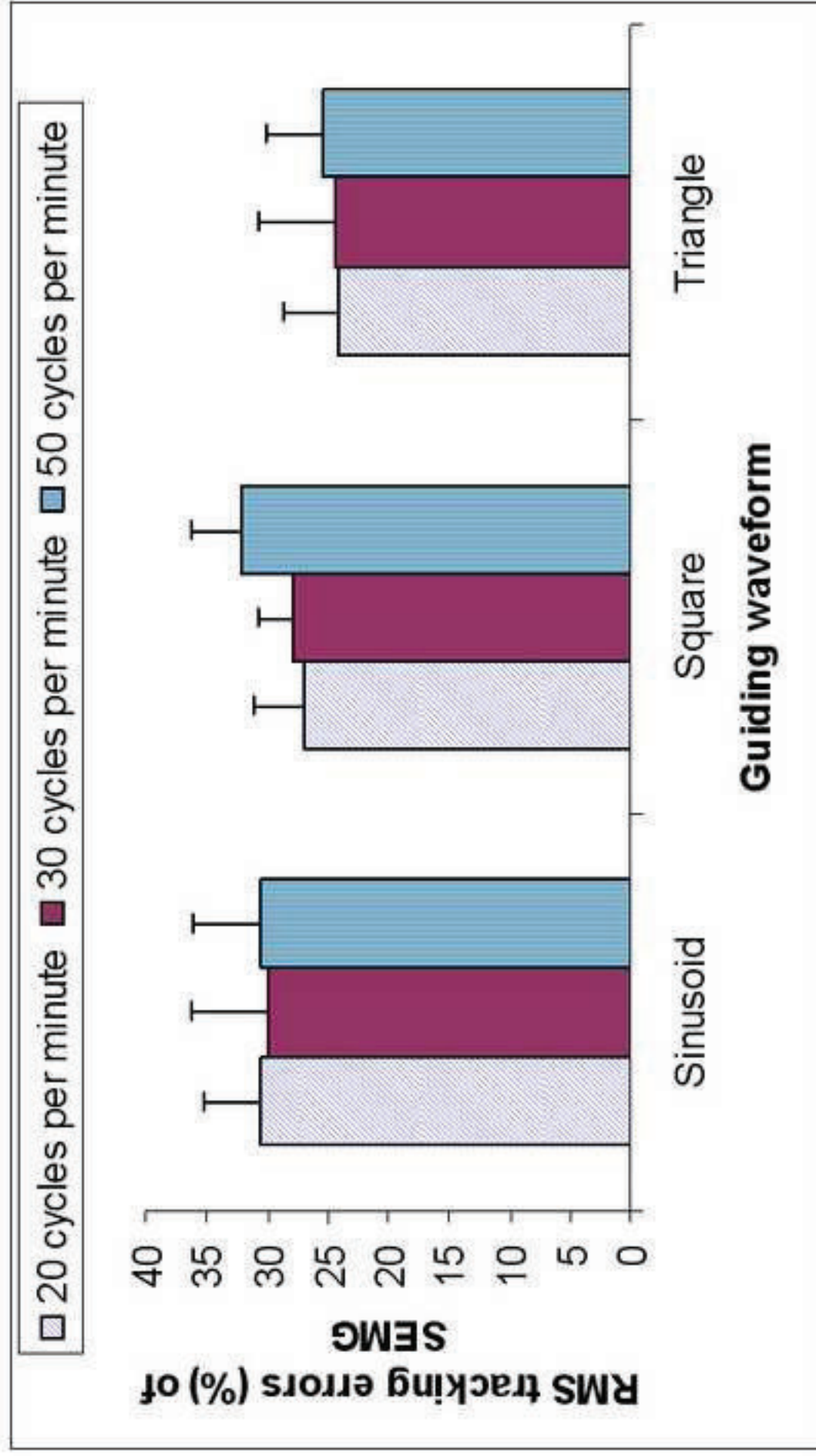


Fig. 7